Available online at www.sciencedirect.com
ScienceDirect
Ceramics International 36 (2010) 1217–1223
CERAMICS INTERNATIONAL
www.elsevier.com/locate/ceramint

Generation of ceramic–ceramic layered composite microstructures using electrohydrodynamic co-axial flow

M. Nangrejo *, Z. Ahmad, M. Edirisinghe

Department of Mechanical Engineering, University College London, Torrington Place, London WC1E 7JE, UK

Received 4 November 2009; received in revised form 13 November 2009; accepted 12 December 2009
Available online 28 January 2010

Abstract

In this work different loading volumes (10 and 20 vol.%) of alumina and zirconia were suspended in selected liquid carriers to prepare suspensions. These suspensions were infused through inner and outer capillaries of a co-axial nozzle arrangement, which was then subjected to an electric field. The rate at which these suspensions were perfused (flow rate) and the applied voltage was varied during the experiments. Under optimal conditions, stable cone and jet formation was achieved for selected co-flowing suspensions which subsequently breaks-up into ceramic–ceramic composite droplets. Thus, droplets containing alumina and zirconia were produced and the resulting relics were collected on quartz substrates. These were sintered at 1200 °C and analysed by optical and scanning electron microscopy. The relic size increased as a function of the volume loading and layered encapsulation (shown using SEM and EDX) of alumina by zirconia and *vice-versa*, using this method, is achievable.

Keywords: Alumina; Zirconia; Suspension; Co-axial; Composite; Jetting; Electrohydrodynamic; Ceramic

1. Introduction

Ceramic–ceramic composites are important engineering materials [1,2]. Alumina-based composites containing dispersions of zirconia generally display superior strength, toughness and wear resistance compared to alumina and consequently there has been considerable interest in them [3,4]. A high-density alumina–zirconia sintered structure (which displays high sintering density, high strength, high toughness, and high hardness) has potential as engineering components and abrasion-resistant materials [5,6]. The addition of zirconia to alumina as a sintering additive has been utilized for the objective of increasing the density of alumina-based ceramics, and this concept of toughening alumina ceramics with dispersions of zirconia particles in a matrix is promising. Such alumina–zirconia composite materials offer higher fracture toughness and mechanical strength [7], which extends their durability and performance.

Alumina–zirconia ceramic composites (prepared from particles) have been investigated as structural materials since the early 1980s [8]. However, the lack of variety and obstacles in processing and forming methodologies has limited their development, and therefore the diversity of applications of these materials. Mixing alumina and zirconia powders followed by pressing and sintering have been routinely used for manufacturing alumina–zirconia composites for many years [9,10]. Other suspension based processing methods, such as slurry coating techniques (for alumina–zirconia) and hot pressing have been used to prepare ceramic composites. The preparation of annular, functionally graded or encapsulated structures of ceramic composites is more difficult to achieve and requires more sophisticated methods or additional steps than physically blending materials together [11–14].

The re-emergence of electrohydrodynamic spraying, spinning and similar fundamental processes to fabricate structures utilising liquids, solutions and suspensions is gathering pace. It is mainly used in painting, fuel atomization in combustion systems, emulsification, microencapsulation, crop spraying and electrostatic scrubbing but in recent times the uses of ceramics in biomedical applications [15–17] has also led to the utilization of such methods. The underlying principle of this process focuses on cone and jet formation using an electric field. The geometrical features of the jet and the various modes

* Corresponding author. Tel.: +440 20 76793920; fax: +440 20 73880180.
E-mail address: m.nangrejo@ucl.ac.uk (M. Nangrejo).

0272-8842/$36.00
doi:10.1016/j.ceramint.2010.01.012

encountered as a function of operating parameters, including the electric field, have been classified into various modes [15]. The main types are dripping, micro-dripping, spindle, multi-spindle, cone-jet, oscillating, precession and multi-jet [15]. The electrohydrodynamic cone-jet mode, which is the most stable mode and also generates a near uniform structure distribution [18], has been used to process ceramic suspensions [19–21]. Subsequently, 3D bio-ceramic direct writing [22], ceramic thin films [23], ceramic foams [24] and nano-ceramic powders [25,26] have been processed in this way. Electrohydrodynamic processing has now extended to incorporate multiple capillaries [26,27] to enable multi-media flow for co-axial jetting [28].

Previously [29] encapsulation of 5 vol.% of alumina by zirconia using a similar method was carried out, and showed encapsulation using low density and viscosity suspensions and in this study the reverse encapsulation (zirconia by alumina) was also not investigated [29]. In this work we explored encapsulation using these suspensions but extended the loading to 10 and 20 vol.% (of both alumina and zirconia) and we also present interchangeable layered ceramic–ceramic (alumina–zirconia or zirconia–alumina) encapsulation by changing the flow in individual capillaries from inner to outer needles and *vice versa*.

2. Experimental details

2.1. Materials

Zirconia powder (Grade HSY3, median particle size 0.4 μm, density 6000 kg m^{-3} supplied by Minchem Chemical Aldershot, U.K) and alumina powder (grade A16.SG, median particle size 0.5 μm, density 3987 kg m^{-3} supplied by ALCOA, Ludwigshafen, Germany) were used. Olive oil (oleocanthal) [(E)-4-hydroxyphenethyl 4-formyl-3-(2-oxoethyl) hex-4-enoate] (density 887 kg m^{-3}) and glycerol (density 1260 kg m^{-3}) were used to suspend the zirconia and alumina, respectively. 1 wt.% of EFKA 4401 (donated by Stort Chemical, Bishop Stortford, U.K., density 950 kg m^{-3}) was used as the dispersant in both suspensions.

2.2. Suspension preparation

Selected ceramic powder (alumina or zirconia) was added in small increments (to prepare the desired loading volume, 10/20 vol %) at a time, to either glycerol or oleocanthal and dispersant, respectively, in a beaker. The beaker containing the desired mixture was mixed and stirred manually after which it was placed in a water bath (20 °C). The partially mixed contents were then subjected to ultrasonic agitation for 1800 s with an input power of 200 W. The water in the surrounding bath was changed every 300 s, and the mixing was carried out at ambient temperature (22 °C). Suspensions containing 10–20% vol. of alumina and zirconia were prepared in this way, and subsequent constant mixing was applied (mechanical rollers) to prevent sedimentation. Suspensions were then sonicated again (200 W, 600 s) just prior to atomization to reduce any sedimentation.

2.3. Suspensions characterization

The density, surface tension, viscosity, electrical conductivity and relative permittivity of the suspensions were measured and were calibrated against glycerol and olive oil, which were used as reference points. The densities of the samples were estimated using a standard density bottle. Surface tension was measured using a Kruss Tensiometer K9 (Krüs GmbH, Hamburg, Germany). Viscosity was measured using a Visco-Easy Rotational viscometer. Electrical conductivity was assessed using a HACH SensION ™ 156 probe (Camlab Ltd., Cambridge, UK). Relative permittivity was measured using the standard capacitance method. All measurements were performed at the ambient temperature.

2.4. Electrohydrodynamic processing

The experimental set-up for co-axial electrodydrodynamic atomization is shown in Fig. 1. The co-axial nozzle device contained an outer needle with internal diameter 850 μm and external diameter 1240 μm, and an inner needle with inner

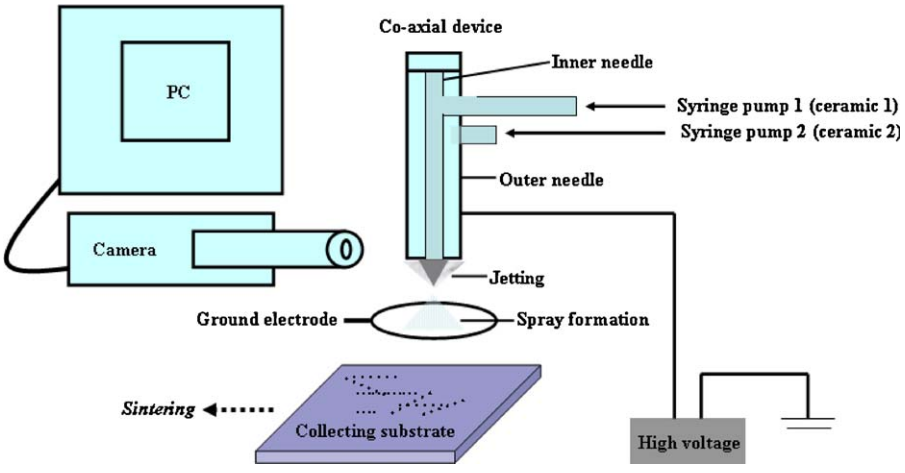

Fig. 1. Schematic set-up for co-axial electrohydrodynamic atomization.

diameter 250 μm and external diameter 460 μm. Outer and inner stainless steel needles were connected to the same voltage supply (Glassman Europe Limited, Bromley, UK) relative to an earthed ring electrode placed 15 mm below the outer needle. The outer diameter of the ring electrode was 20 mm and the inner diameter was 15 mm. Flow of suspensions of alumina/glycerol and zirconia/oleocanthal were controlled by two precision Harvard syringe pumps (Harvard Apparatus Ltd., Edenbridge, UK) using 10 mL syringes. Co-flow behaviour of alumina/glycerol and zirconia/oleocanthal suspensions from the inner needle and outer needle were observed using a LEICA S6D JVC-coloured video camera attached to a zoom lens and a data DVD video recorder. Jet length (L) and diameter (D) were measured from recorded information using computer software (JEOL SemAfore V.4).

The experiments were carried out at the ambient temperature. First, alumina (10/20 vol.%) suspension was pumped through the inner needle at flow rates between 20 and 100 μL/min. To demonstrate the processing jetting modes, a mode-selection map was constructed based on the flow rate and the applied voltage. To elucidate high volume ceramic–ceramic layering, zirconia (10/20 vol.%) suspension was infused through the outer needle at flow rates 40–200 μL/min, whilst maintaining the initial flow of alumina suspension through the inner needle. The flow rate ratio (inner: outer needle) between the needles was kept at 1:2 respectively, and this allowed the formation of a co-flow jetting mode map. Selected permutations were carried out with changes made to the placement of flowing materials e.g. location in inner and outer needles. For example, in one set of experiments, 10 vol.% alumina was perfused through in the inner needle and 10 vol.% zirconia was used in the outer needle, after which their locations were switched over. Similarly, 20 vol.% suspensions of both ceramics were subject to co-flow in similar fashion. The flow rate and applied voltage were varied until optimal conditions (stable and prolonged jetting) were determined. The jet break-up generated many fine droplets and samples of these were collected on a quartz slide (UQG Optics Ltd., Cambridge, UK). It is possible to collect these structures in liquid phases [27], which reduces the deformation of particles, however as the particles were to be subject to sintering, they were collected directly on to the sintering substrate.

2.5. Sintering

Samples were sintered in a muffle furnace by heating from the ambient temperature to 1200 °C at 30 °C min^{-1}, followed by soaking at this temperature for 3600 s. The samples were cooled in the furnace to ambient temperature by switching off the heating.

2.6. Characterization

Droplets relics were investigated before and after heat treatment using optical microscopy. Furthermore, the sintered relics were investigated by JEOL JSM 3600 scanning electron microscopy. Samples were coated with a thin layer of carbon before examination.

3. Results and discussion

3.1. Suspension and jet behaviour

The 10/20 vol.% alumina and zirconia suspensions, used in the preparation of layered ceramic–ceramic microstructures using electrohydrodynamic co-flow, were characterized and assessed for their processing suitability. The properties of the suspensions and liquids which influence electrohydrodynamic processes are shown in Table 1. Jet formation and stability depend largely on the electrical conductivity and surface tension characteristics of the powder and the liquid in which it is suspended [26,30]. For co-flowing systems at least one material must show electrical conductivity [31] in order to permit jet formation. Subsequently, materials with high surface tension values may also hinder stable jet formation, although there are several strategies in place to overcome this [32]. In this work, there results a large difference in the surface tension between different loading volumes of the same suspensions e.g. alumina (10/20 vol.%: 54–110 mN/m, respectively) and zirconia (10/20 vol.%: 48–82 mN/m respectively). In comparison with other studies utilising ceramic suspensions for electrohydrodynamic processing [16,29] the 10 vol.% suspensions shows surface tension properties which make them suitable for stable-jetting. Higher loading volumes (20 vol.%) have increased surface tension, which suggests there may be intermittent instabilities during the jetting process. Zirconia suspensions have lower electrical conductivities ($\ll$1 S/m) when compared to alumina suspensions and this is due to the suspensions being prepared from olive oil, which is an insulator. However, co-flow will be possible as glycerol (carrier medium for alumina) has a much higher electrical conductivity and will therefore be the driving medium, permitting the jetting process [31]. Viscosities of the suspensions also increased as a function of the loading volume e.g. alumina (10/20 vol.% alumina: 1150/1820 mPa s, respectively) and zirconia (10/20 vol.%: 480/875 mPa s, respec-

Table 1
Physical properties of liquids and suspensions used.

Property	Alumina 10 vol.%	Alumina 20 vol.%	Zirconia 10 vol.%	Zirconia 20 vol.%	Alumina 5 vol.% (Ref. [29])	Zirconia 5 vol.% (Ref. [29])	Olive oil	Glycerol
Density (kg/m^3)	1510	1902	1442	1710	1424	1168	887	1260
Surface tension (mN/m)	54	110	48	82	66	37	42	65
Viscosity (mPa s)	1150	1820	480	875	1120	107	80	988
Electrical conductivity (S/m)	9×10^{-5}	11×10^{-5}	$\ll$1	$\ll$1	5×10^{-5}	4×10^{-6}	$\ll$1	20

tively). The quantity of material dissolved or suspended in the liquid carrier medium (which also determines the mediums viscosity) can influence the size of the structures generated [33].

3.2. Atomization modes

Under the influence of an electric field and providing the physical properties of the media fit the criteria mentioned, suspensions emerging from the needle exit can undergo various modes of atomization as a function of the applied voltage [30,34]. This is highlighted in Fig. 2. For this 10 vol.% suspensions of alumina and zirconia were selected. Alumina suspension was perfused through the inner needle at a flow rate of 80 μL/min and as the liquid collected at the inner needle exit it concealed both needles during droplet formation (Fig. 2a). With the application of voltage (2.5 kV) the droplet size was smaller with increased rate of dripping (Fig. 2b). Once the applied voltage reached 5.3 kV the stable-jetting mode was achieved. At this point, the zirconia suspension was perfused through the outer needle at 160 μL/min, and this initial flow of zirconia suspension from the outer needle is shown in Fig. 2c. However, once the flow of zirconia had stabilized (constant rate), stable-jetting of co-flow media (both 10 vol.% suspensions) ceased to exist at the same voltage (Fig. 2d), and is more reminiscent of dripping modes [35]. Increasing the voltage during electrohydrodynamic co-flow from 5.3 to 9.6 kV results in the spindle mode. This displays a cone-jet, but the jet is not stable and undergoes rotary motion at skewed angles from the cone (Fig. 2e). Adjusting the applied voltage from 9.6 to 10.4 kV results in stable-jetting, as shown in Fig. 2f, which is the mode required to prepare layered ceramic–ceramic microstructures.

3.3. Effect of applied voltage and flow rate on jetting modes

Fig. 3a and b show mode-selection (M-S) maps, which are constructed to define parametric effects on generating the

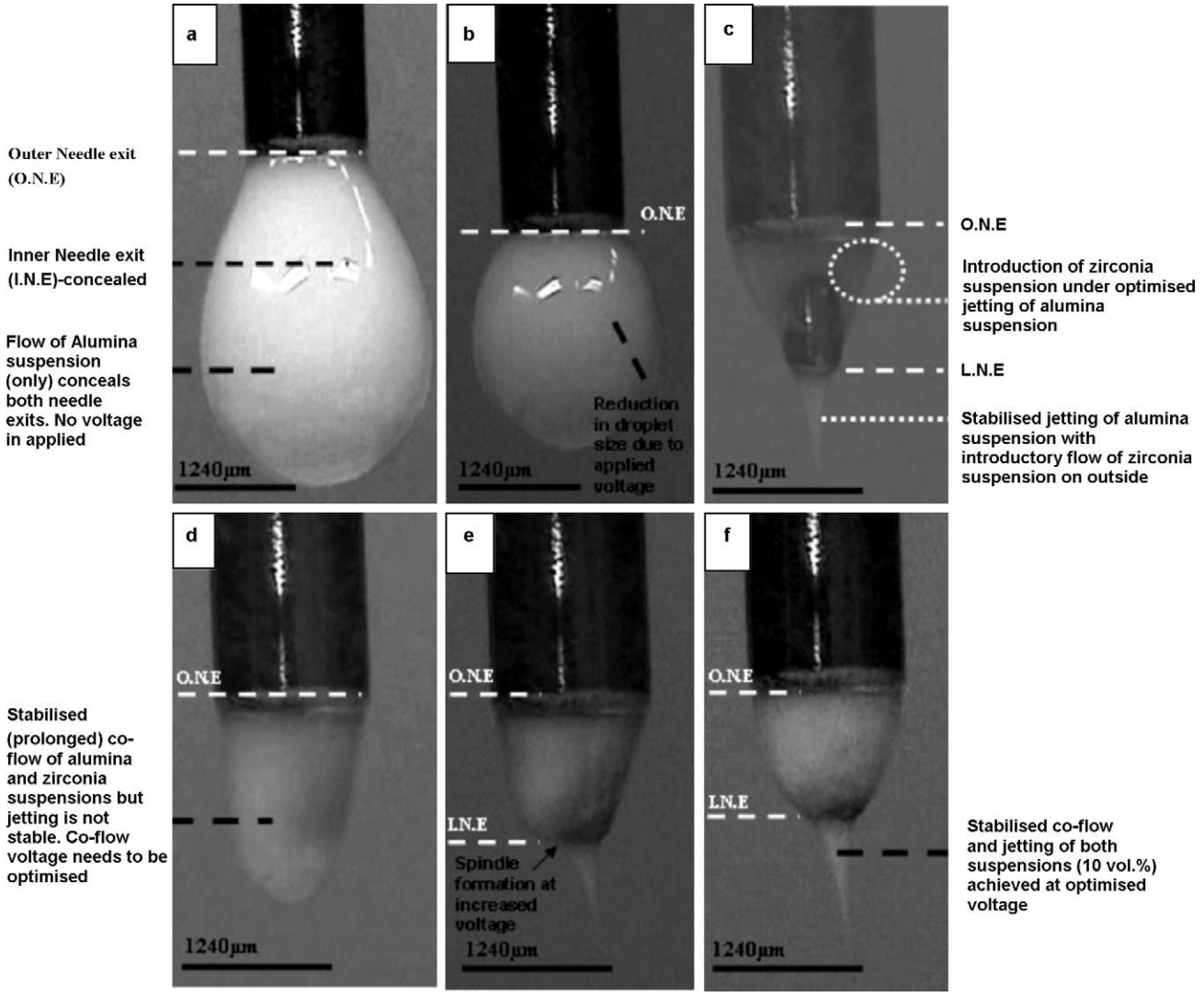

Fig. 2. Examples of atomization jetting modes showing alumina suspension (10 vol.%) exiting the inner co-axial needle (flow rate 80 μL/min) at (a) 0 kV (b) 2.5 kV (c) 5.3 kV with the initial flow (160 μL/min) of zirconia suspension (10 vol.%) through the outer co-axial needle. Stabilized (regular) co-axial flow of both suspensions at (d) 5.3 kV (e) 9.6 kV and (f) 10.4 kV.

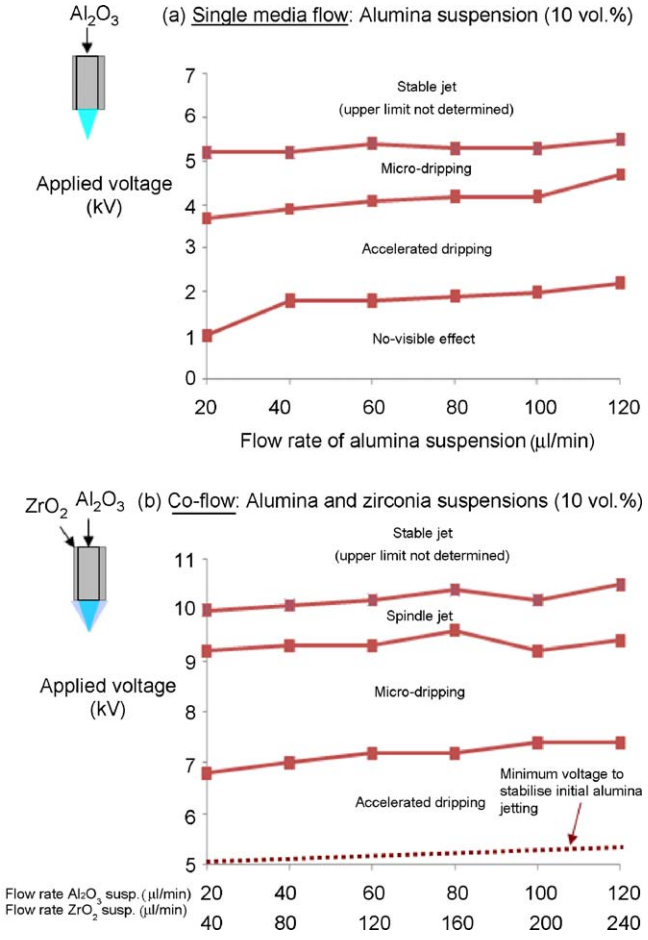

Fig. 3. Mode-selection maps for (a) 10 vol.% of alumina suspension flowing through the inner co-axial needle at parameters 0–6 kV and 20–120 μL/min. Mode-selection map for (b) co-flowing suspensions (both 10 wt%) under stabilized flow (after initial flow of zirconia to stable-jetting with alumina) at parameters 6–11 kV and outer needle flow rates twice that of those the established inner needle (inner needle 20–120 μL/min, outer needle 40–240 μL/min).

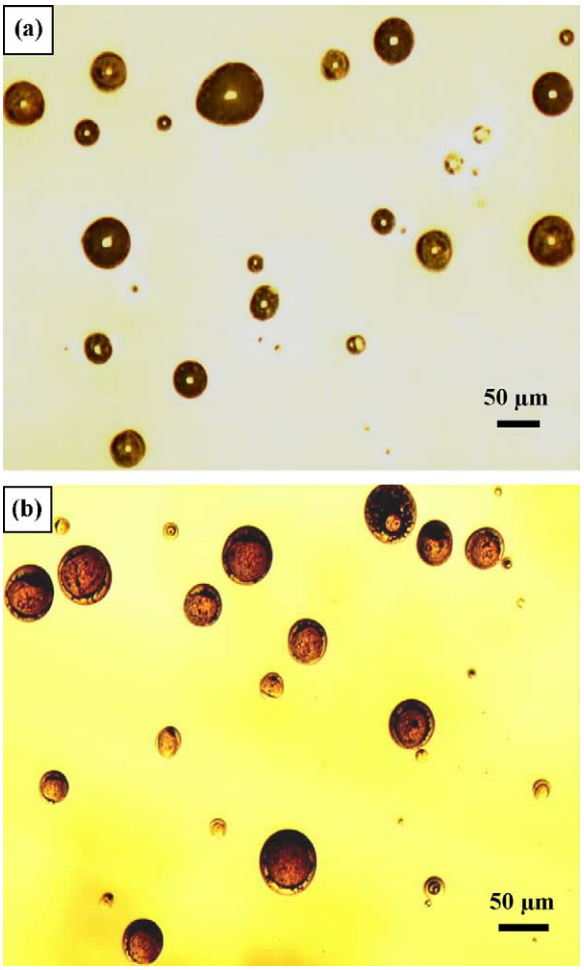

Fig. 4. Optical micrographs of relics generated (before sintering using) 10 vol.% suspensions during stabilized co-flow jetting, showing (a) alumina (inner needle) layered with zirconia and (b) zirconia (inner needle) layered with alumina.

various jetting modes. To elucidate this, 10 vol.% suspensions were used in similar fashion as described above. However, the flow rates were increased gradually; with the flow of media from the outer needle twice that of the inner needle. The applied voltage was increased stepwise at each flow rate adjustment and the jetting mode was observed. It is noteworthy that a flow rate of 80 μL/min enabled prolonged flow and flow rates below this value (for the inner needle), may not represent flow of the perfusor input rate. Fig. 3a shows the M-S map of single media flow (alumina suspension from the inner needle) and at all flow rates the stable-jetting mode was achieved at an applied voltage just 5–5.3 kV. Introducing zirconia suspension through the outer needle while jetting the stabilized alumina suspension (5–5.3 kV) results in co-flow of ceramic suspensions. Mapping this co-flow (Fig. 3b) shows that the spindle mode results just prior to the stable co-flow jetting mode. The upper limit of the stable-jetting mode was not determined where other modes can manifest, such as multi-jetting [18], and these are not required for this work.

3.4. Structure analysis

Structures obtained (non-sintered) from stable-jetting of co-flowing ceramic suspensions (10 vol.%) are shown in Fig. 4. Fig. 4a shows alumina encapsulated with zirconia obtained at an applied voltage of 10.4 kV (alumina suspension inner needle: 80 μL/min, zirconia suspension outer needle: 160 μL/min). The mean size is 32 μm with a range of 9–55 μm (excluding satellite particles which are due to the outer medium only). Reversing the location of the co-flowing media (alumina: outer needle, zirconia: inner needle) also results in relics with a layered structure. However, to generate these, the voltage required to enable a stable jet was lower at the same needle flow rate conditions (9.2 kV). These had a mean size of 36 μm with a range of 13–52 μm. Compared to the earlier study focusing on 5 vol.% suspensions [29], even though the present structures have a higher loading volume, they are still smaller in size (mean size 120 μm reported earlier). Generally, it is anticipated that higher loading volumes will generate larger structures. In this study the generation of smaller structures (from 10 vol.% suspensions) could be explained due to the increased sonication

time during suspension preparation, and also sonication just prior to processing, which was not present in the earlier study. The other difference, which may not contribute towards the difference in morphology size, is the co-flow rates. In this work the outer needles flow rate was kept at twice the speed of the inner needles, and this was essential to allow prolonged flow from both needles.

The more viscous suspensions of alumina and zirconia (20 vol.%) were also subjected to co-flow atomization, but required higher flow rates to enable constant flow of media. The flow rates of the inner and outer needles for these concentrated suspensions were 120 and 240 μL/min, and even at these speeds there was intermittent needle blockage. In the first instance (Fig. 5a), alumina suspension was perfused through the inner needle and zirconia was perfused through the outer needle at the aforementioned flow rates. The voltage required to enable stable-jetting was 14.8 kV, which is appreciably higher than that required for 10 vol.% suspensions. The structures are shown after sintering at 1200 °C in Fig. 5a1 and a2. These had a mean size of 125 μm with a range of 80–125 μm. These structures are larger than those obtained for the 10 vol.% suspensions even after sintering, which may cause some shrinkage. To confirm the location of the individual ceramics, EDX analysis was carried out on selected locations of a sintered structure (Fig. 5a3). Analysis at the edge of this structure (Fig. 5a3, point Y) shows there is a much larger concentration of zirconia when compared to alumina. In contrast, analysis at the centre of the structure (Fig. 5a3, point X) reveals a higher concentration of alumina when compared to zirconia. This, the microscopic evidence suggests layered ceramic–ceramic composites were generated. Reversing the location of media flow also results in layered ceramic structures. For example perfusing 20 vol.% zirconia in the inner needle and alumina in the outer needle, at the same flow rates but requiring an applied voltage of 13.5 kV generates layered morphologies. Fig. 5b1 and b2 show examples of sintered (1200 °C) structures. These had a mean size of 83 μm with a range of 30–125 μm. EDX analysis at two points (Fig. 5b3) of a selected sintered structure

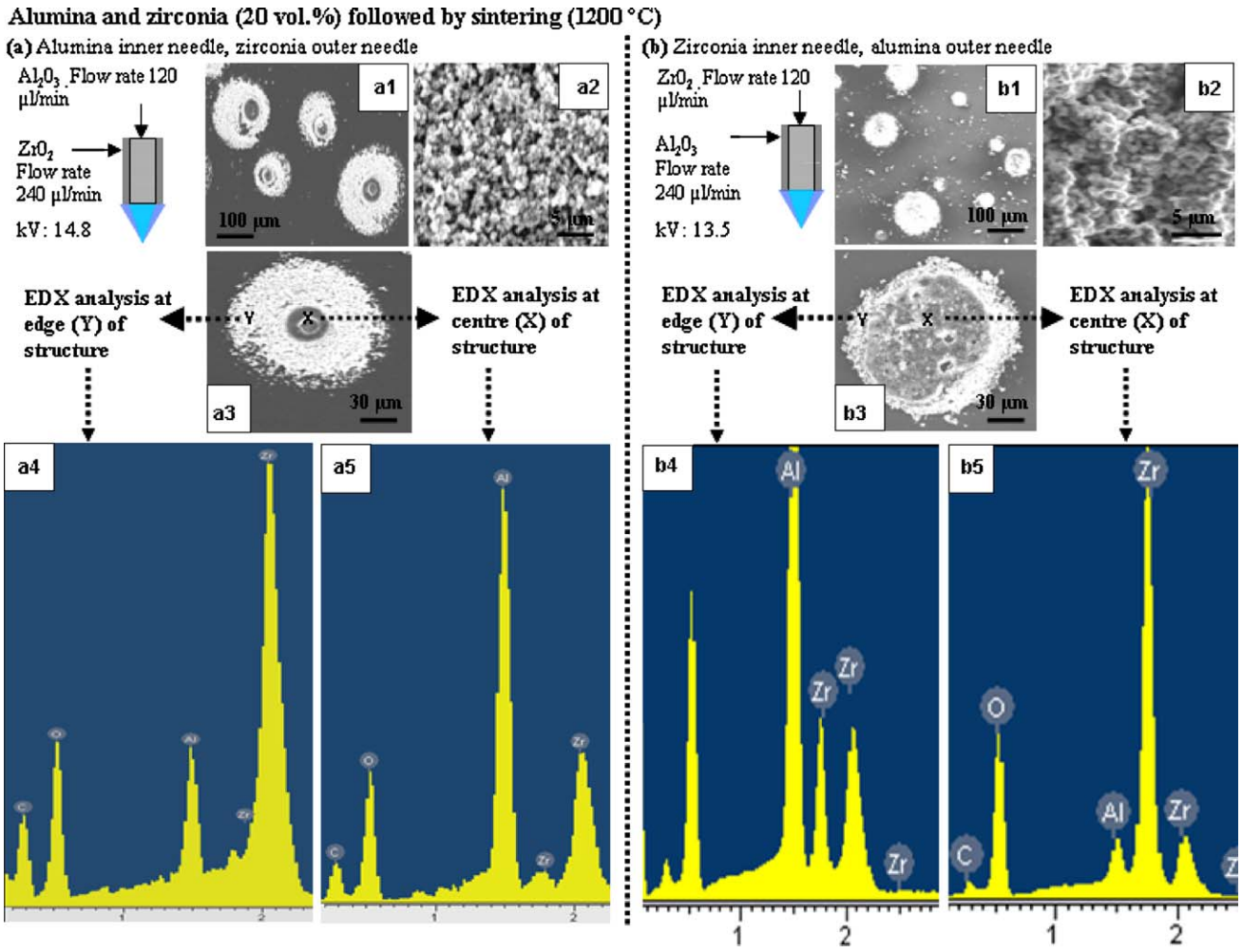

Fig. 5. Sintered (1200 °C) structures prepared using 20 vol.% suspensions analysed used scanning electron microscopy and EDX. Examples of alumina layered with zirconia shown in micrographs at (a1) low magnification and (a2) high magnification at the edge and (a3) structure used for EDX analysis. EDX analysis of structure at (a4) Y-edge and (a5) X-centre. Examples of zirconia layered with alumina shown in micrographs at (b1) low magnification and (b2) high magnification at the edge and (b3) structure used for EDX analysis. EDX analysis of structure at (b4) Y-edge and (b5) X-centre.

shows the difference in composition between the centre and the edge of the structures (Fig. 5b4 and b5), which again demonstrates ceramic–ceramic layering.

4. Conclusions

In this paper, a co-axial electrohydrodynamic jetting process was carried out using concentrated alumina and zirconia suspensions (10 and 20 vol.%). Experimental results show that alumina and zirconia layered encapsulation is possible using this method, generating novel ceramic–ceramic composite microstructures. The layered structure size increases as a function of the loading volume, but compared with an earlier study may also depend on how well the particles are suspended just prior to processing. However, concentrated suspensions require higher flow rates to enable prolonged flow and jetting, but still exhibit instabilities during jetting. One way to overcome this may be to use much coarser needles or capillaries. This novel process offer exciting possibilities for encapsulating micro and nano scaled materials to produce novel composites for engineering, drug delivery and bioengineering applications.

Acknowledgements

The authors wish to thank the Leverhulme Trust (Grant: F/07 134/BL) and EPSRC (EP/E045839) for supporting this work. They would also like to thank the Archaeology Department (UCL) for the use of their electron microscopes.

References

[1] Z. Wang, J. Shemilt, P. Xiao, Novel fabrication technique for the production of ceramic/ceramic and metal/ceramic composite coatings, Scripta Mater. 42 (2000) 653–659.
[2] F. Wang, K. Zhang, G. Wang, Texture in superplastically deformed alumina–zirconia composites, Mater. Sci. Eng. A 491 (2008) 476–482.
[3] Z. Wang, J. Shemilt, P. Xiao, Fabrication of ceramic composite coatings using electrophoretic deposition, reaction bonding and low temperature sintering, J. Eur. Ceram. Soc. (2002) 183–189.
[4] S. Mirhashemi, H. Baharvandi, H. Abdizadeh, N. Ehsani, Effects of processing temperature and fabrication method on microstructure and density of multilayer Al_2O_3–ZrO_2 nanocomposites, Int. J. Mod. Phys. A. 22 (2008) 3254–3260.
[5] F. Cesari, L. Esposito, F.M. Furgiuele, C. Maletta, A. Tucci, Fracture toughness of alumina–zirconia composite, Ceram. Int. 32 (2006) 249–255.
[6] T.S. Suzuki, Y. Sakka, K. Kitazawa, Texture development in zirconia-dispersed alumina composites by slip casting in a high magnetic field, Appl. Superconductivity Trans. 14 (2004) 1584–1587.
[7] C. Maria, Mechanical properties of alumina–zirconia composites for ceramic abutments, Mater Res. 7 (2004) 643–649.
[8] R.W. Rice, A material opportunity: ceramic composites, Chemtec 13 (1983) 230–239.
[9] C. Laurent, A. Rousset, P. Bonneford, D. Oquab, B. Lavelle, Mechanical properties of alumina-metal-zirconia nano-micro hybrid composites, J. Eur. Ceram. Soc. 16 (1996) 937–943.
[10] F.J. Zhang, F.X.Y. Yang, L. Huang, D.G. Zhu, The character of sintering under vacuum and its use in hot isostatic pressing in comparison with the air pre-sintering and slurry coating techniques for alumina–zirconia composites, J. Mater. Process. Technol. 74 (1998) 115–121.
[11] S. Battacharya, K. Jacus, Hot pressing of annular alumina–zirconia composites, J. Am. Ceram. Soc. 81 (1998) 460–464.
[12] M. Mott, J.R.G. Evans, Zirconia/alumina functionally graded material made by ceramic ink jet printing, Mater. Sci. Eng. A 271 (1999) 344–352.
[13] X.D. Li, L. Wang, T. Onda, T. Akao, M. Hayakewa, Fabrication of Al_2O_3–ZrO_2(3Y-TZP) composites with graded structures by centrifugal slip casting method, Mater. Sci. Forum 449 (2004) 293–296.
[14] A. Mattern, R. Oberacker, M.J. Hoffman, Multi-phase ceramics by computer-controlled pressure filtration, J. Eur. Ceram. Soc. 24 (2004) 3219–3225.
[15] A. Jaworek, A. Krupa, Jet and drops formation in electrhydrodynamic spraying of liquids. A system approach, Exp. Fluids 27 (1999) 43–52.
[16] Z. Ahmad, E.S. Thian, J. Huang, M.J. Edirisinghe, S.N. Jayasinghe, D.C. Ireland, R.A. Brooks, N. Rushton, W. Bonfield, S.M. Best, Deposition of nano-hydroxyapatite particles utilising direct and transitional electrohydrodynamic processes, J. Mater. Sci. Mater. M. 19 (2008) 3093–3104.
[17] M. Nangrejo, Z. Ahmad, P. Colombo, E. Stride, M.J. Edirisinghe, Preparation of polymeric and ceramic porous capsules by a novel electrohydrodynamic process, Pharm. Dev. Technol. 13 (2008) 425–432.
[18] M. Cloupeau, B. PrunetFoch, Electrostatic spraying of liquids: main functioning modes, J. Electrostat. 25 (1990) 165–184.
[19] W.D. Teng, Z.A. Huneiti, W. Machowski, J.R.G. Evans, M.J. Edirisinghe, W. Balachandran, Towards particle-by-particle deposition of ceramics using electrostatic atomization, J. Mater. Sci. Lett. 16 (1997) 1017–1019.
[20] S.N. Jayasinghe, M.J. Edirisinghe, T. De Wilde, A novel ceramic printing technique based on electrostatic atomization of a suspension, J. Mater. Res. Innov. 6 (2002) 92–95.
[21] S. Jayasinghe, M.J. Edirisinghe, Electrostatic atomization of a ceramic suspension, J. Eur. Ceram. Soc. 24 (2004) 2203–2213.
[22] J. Huang, S.M. Best, W. Bonfield, R.A. Brooks, N. Rushton, S.N. Jayasinghe, M.J. Edirisinghe, In-vitro assessment of the biological response to nano-sized hydroxyapatite, J. Mater. Sci. Mater. M. 15 (2004) 441–445.
[23] W. Balachandran, P. Miao, Electrospray of fine droplets of ceramic suspensions for thin-film preparation, J. Electrostat. 50 (2001) 249–263.
[24] S.N. Jayasinghe, M.J. Edirisinghe, A novel method of forming open cell ceramic foam, J. Porous Mater. 9 (2002) 265–273.
[25] S.N. Jayasinghe, R. Dorey, M.J. Edirisinghe, Z.B. Luklinska, Preparation of lead zirconate titanate nano-powder by electrohydrodynamic atomization, J. Appl. Phys. A 80 (2005) 723–725.
[26] Z. Ahmad, H.B. Zhang, U. Farook, M. Edirisinghe, E. Stride, P. Colombo, Generation of multi-layered structures for biomedical applications using a novel tri-needle co-axial device and electrohydrodynamic flow, J. R. Soc. Interface 5 (2008) 1255–1261.
[27] Z. Ahmad, M. Nangrejo, M. Edirisinghe, E. Stride, P. Colombo, H. Zhang, Engineering a material for biomedical applications with electric field assisted processing, Appl. Phys. A 97 (2009) 31–37.
[28] M. Enayati, Z. Ahmad, E. Stride, M. Edirisinghe, One-step electrohydrodynamic production of drug-loaded micro- and nanoparticles, J. R. Soc. Interface (2010), doi:10.1098/rsif.2009.0348.
[29] K. Balasubramanian, S.N. Jayasinghe, M.J. Edirisinghe, Co-axial electrohydrodynamic atomization of ceramic suspensions, Int. J. Appl. Ceram. Technol. 3 (2006) 55–60.
[30] M. Cloupeau, B. Prunet-Foch, Electrostatic spraying of liquids in the cone-jet mode, J. Electrostat. 22 (1989) 135–159.
[31] I.G. Loscertales, A. Barrero, I. Guerrero, R. Cortijo, M. Marquez, A.M. Gañán-Calvo, Micro/nano encapsulation via electrified co-axial liquid jets, Science 295 (2002) 1695–1698.
[32] J.L. Li, A. Tok, Electrospraying of water in the cone-jet mode in air at atmospheric pressure, Intern. J. Mass Spectrom. 272 (2008) 199–203.
[33] M. Enayati, Z. Ahmad, E. Stride, M. Edirisinghe, Preparation of polymeric carriers for drug delivery with different shape and size using an electric jet, Curr. Pharmaceut. Technol. 10 (6) (2009) 600–608.
[34] D.Z. Wang, S.N. Jayasinghe, M.J. Edirisinghe, Z.B. Luklinska, Co-axial electrohydrodynamic direct writing of nano-suspensions, J. Nanopart. Res. 9 (2007), 825, 831.
[35] I. Hayati, A.I. Bailey, T.F. Tadros, Mechanism of stable jet formation in electrohydrodynamic atomization, Nature 319 (1986) 41–43.